

CASP4/caspase-11 promotes autophagosome formation in response to bacterial infection

Kathrin Krause^a, Kyle Caution^a, Asmaa Badr^a, Kaitlin Hamilton^a, Abdulmuti Saleh^a, Khushbu Patel^a, Stephanie Seveau^a, Luanne Hall-Stoodley^a, Rana Hegazi^a, Xiaoli Zhang^b, Mikhail A. Gavrilin^c, and Amal O. Amer^a

^aDepartment of Microbial Infection and Immunity, Infectious Diseases Institute, Columbus, OH, USA; ^bCenter for Biostatistics, The Ohio State University, Columbus, OH, USA; ^cDepartment of Internal Medicine, The Ohio State University, Columbus, OH, USA

ABSTRACT

CASP4/caspase-11-dependent inflammasome activation is important for the clearance of various Gram-negative bacteria entering the host cytosol. Additionally, CASP4 modulates the actin cytoskeleton to promote the maturation of phagosomes harboring intracellular pathogens such as *Legionella pneumophila* but not those enclosing nonpathogenic bacteria. Nevertheless, this non-inflammatory role of CASP4 regarding the trafficking of vacuolar bacteria remains poorly understood. Macroautophagy/autophagy, a catabolic process within eukaryotic cells, is also implicated in the elimination of intracellular pathogens such as *Burkholderia cenocepacia*. Here we show that CASP4-deficient macrophages exhibit a defect in autophagosome formation in response to *B. cenocepacia* infection. The absence of CASP4 causes an accumulation of the small GTPase RAB7, reduced colocalization of *B. cenocepacia* with LC3 and acidic compartments accompanied by increased bacterial replication *in vitro* and *in vivo*. Together, our data reveal a novel role of CASP4 in regulating autophagy in response to *B. cenocepacia* infection.

ARTICLE HISTORY

Received 30 May 2017
Revised 6 June 2018
Accepted 13 June 2018

KEYWORDS

autophagy; *Burkholderia cenocepacia*; caspase-1 (CASP1); caspase-11 (CASP4); lysosome; macrophages

Introduction

Autophagy, an intracellular catabolic pathway, is a highly regulated stress response that ensures cellular homeostasis and provides protection against harmful conditions. Typical stimuli known to induce autophagy are nutrient deprivation, increased production of reactive oxygen species, and the accumulation of protein aggregates. The breakdown of damaged organelles and proteins via autophagy leads to the recycling of nutrients and sustains cellular energy levels. In addition, autophagy targets various intracellular pathogens such as *Mycobacterium tuberculosis* [1], *Salmonella enterica* serovar Typhimurium [2], *Legionella pneumophila* [3], *Streptococcus pyogenes* [4], and *Burkholderia cenocepacia* [5]. This bacteria-specific autophagic process, designated xenophagy, promotes bacterial clearance and prevents cellular escape. Bacteria such as *Listeria monocytogenes* [6,7] or *Burkholderia pseudomallei* [8], although recognized by members of the autophagic pathway, have developed mechanisms to avoid lysosomal degradation and xenophagy.

B. cenocepacia, commonly found in soil and water, is a Gram-negative facultative intracellular pathogen that causes severe infections among immune-deficient individuals, particularly patients with cystic fibrosis (CF) or chronic granulomatous disease [9–11]. We and others found that defective autophagy is responsible for the persistence of *B. cenocepacia* within eukaryotic cells. Maturation of the *B. cenocepacia*-containing vacuole (BCV) is delayed in murine RAW 264.7

macrophages, yet delivery to lysosomes still occurs and infection is restricted [12]. In contrast, CFTR (cystic fibrosis transmembrane conductance regulator) $\Delta F508$ macrophages from human and mice are permissive to *B. cenocepacia* due to inefficient fusion of the BCV with lysosomes. Therefore, it can be concluded that defective autophagy promotes survival of *B. cenocepacia* in professional phagocytes. However, pharmacological stimulation of autophagy prior to infection restores bacterial delivery to acidic lysosomal compartments, thereby improving degradation of *B. cenocepacia* within murine CF macrophages [5]. Human macrophages derived either from patients with CF or chronic granulomatous disease also show improved restriction of *B. cenocepacia* after treatment with the autophagy-inducing agent rapamycin [13,14].

Alongside autophagy, inflammasome assembly is a crucial mechanism for innate immune cell defense against invading pathogens. Activation of CASP1/caspase-1 within a molecular platform comprising cytosolic NOD-like receptors (NLRs) and various adaptor proteins drives the secretion of pro-inflammatory cytokines such as IL1 β /IL-1 β (interleukin 1 beta) and IL18, which can be accompanied by plasma membrane disruption and host cell death (pyroptosis). As part of the non-canonical inflammasome, CASP4/caspase-11 contributes to cytokine release and bacterial restriction either upstream or independently of CASP1 [15–18]. *B. cenocepacia* activates CASP1 via NLRP3 in murine macrophages [19] and via MEFV/PYRIN in human monocytes [20] in a type VI

secretion system (T6SS)-dependent manner, resulting in pronounced inflammation. A potential role for CASP4 during *B. cenocepacia* infection, however, has not yet been investigated.

Whereas cross-talk between autophagy and inflammasomes has been reported by several groups, these studies mostly report that autophagy negatively regulates inflammasome signaling to prevent excessive inflammation [21–23]. However, during *L. pneumophila* infection, inflammasome activation promotes autophagy [24]. Specifically, CASP4 activity modulates actin polymerization in *L. pneumophila*-infected macrophages, and hence facilitates the trafficking of phagosomes to lysosomal compartments for bacterial clearance [16,25]. Interestingly, transportation of phagosomes containing nonpathogenic *Escherichia coli* is not influenced by CASP4, suggesting differential regulation of endocytic pathways depending on the captured cargo [16]. Nonetheless, it remains unclear if CASP4 plays a role for the trafficking of other pathogenic bacteria such as *B. cenocepacia*.

Here we demonstrate that CASP4 positively regulates autophagosome formation and trafficking to lysosomes in murine macrophages. CASP4 deficiency leads to increased replication of *B. cenocepacia* in murine macrophages *in vitro* and infected lungs accompanied by elevated bacterial dissemination to the spleen *in vivo*. Furthermore, transport of *B. cenocepacia* to phagosomes, the precursors to autophagosomes, and subsequent delivery to lysosomes is compromised in *casp4*^{-/-} macrophages resulting in the accumulation of RAB7, a small GTPase that is involved in phagosome maturation and acidification [26]. Our findings provide new insights into non-pyrototic functions of CASP4 by facilitating autophagosome biogenesis and trafficking in response to intracellular pathogens.

Results

CASP4 contributes to the restriction of *B. cenocepacia* and the release of cytokines *in vitro*

CASP4 restricts the growth of *L. pneumophila*, an intracellular pathogen that resides in autophagosomes in WT macrophages [3,16,25]. Notably, *B. cenocepacia* is also cleared by autophagosomes in healthy macrophages [5], but the role of CASP4 in intracellular trafficking of this bacterium is not known. In order to determine whether CASP4 is involved in the restriction of *B. cenocepacia*, we infected bone marrow-derived macrophages from C57BL/6 wild-type (WT) and *casp4*^{-/-} mice and examined intracellular bacterial growth. Compared to WT macrophages, we found an approximately 1.9-fold increase in colony forming units (CFUs) at 6 h post infection in the absence of CASP4 (Figure 1a and S1A). When the numbers of intracellular bacteria was analyzed via confocal microscopy, a higher proportion of *casp4*^{-/-} macrophages contained > 5–10 bacteria/cell compared to WT cells at 6 h post infection (Figure 1b and c). Accordingly, significantly more WT macrophages contained < 5 bacteria/cell (Figure 1c), suggesting that bacterial clearance is more effective in WT macrophages. In order to determine the amount of cell death in response to *B. cenocepacia* infection, we measured the release of LDH (lactate dehydrogenase) from WT

and *casp4*^{-/-} macrophages at 6 h post infection. Single *casp1*^{-/-} macrophages that are defective in pyroptosis, were included as a control. We found lower levels of LDH in the supernatants from *casp4*^{-/-} and *casp1*^{-/-} macrophages, but overall cell death was low in all 3 genotypes (Figure 1d).

Basal expression of CASP4 is low in resting cells and its expression and activity are triggered by bacterial factors such as intracellular lipopolysaccharide [27,28]. To determine if *B. cenocepacia* infection of WT macrophages induces CASP4 protein expression, macrophages were infected with bacteria for 2 h or 6 h and the expression of CASP4 was evaluated by immunoblot. Like other Gram-negative bacteria, *B. cenocepacia* induced the expression of CASP4 in WT macrophages with an ~ 1.7-fold increase at 2 h (Fig. S1B-C) and a 6-fold increase at 6 h compared to non-infected control cells (Figure 1e and g). Because CASP4 stimulates non-canonical NLRP3 inflammasome activation in response to Gram-negative bacteria [15], we further analyzed if CASP4 contributes to *B. cenocepacia*-induced CASP1 activation. The processing of CASP1 in WT and *casp4*^{-/-} macrophages was compared via immunoblot. As shown in Figure 1f-g and S1D, proteolytic cleavage of CASP1 after *B. cenocepacia* infection is significantly decreased in *casp4*^{-/-} macrophages, indicating a crucial role for CASP4 in *B. cenocepacia*-mediated inflammasome activity.

To determine if CASP4 also modulates the secretion of IL1B in response to *B. cenocepacia*, we measured the amount of released IL1B from macrophages at 6 h post infection using *casp1*^{-/-} macrophages as a control. Figure 1h and S1E show that CASP4 deficiency resulted in significantly decreased production of IL1B. Interestingly, *casp4*^{-/-} macrophages also produced lower levels of the inflammasome-independent cytokine IL1A (interleukin 1 alpha) and the chemokine CXCL1/KC (analog of human CXCL8/IL8) (Figure 1h). In contrast, the absence of CASP1 was not associated with decreased CXCL1/KC secretion.

Because CASP7 (caspase 7) is a known substrate of CASP1 [29,30], we further evaluated if CASP4 affected CASP7 activation. Indeed, *B. cenocepacia* induced cleavage of CASP7 in WT macrophages, which was significantly reduced in *casp4*^{-/-} macrophages (Fig. S1F-G). Therefore, these results show that CASP4 restricts the growth of *B. cenocepacia* and modulates the release of cytokines and the activation of CASP1 and CASP7 in macrophages.

CASP4 is expressed in *mefv*^{-/-}/*pyrin*^{-/-} macrophages with reduced activation of CASP1 in response to *B. cenocepacia*

Because the PYRIN inflammasome also plays a role in the detection of *B. cenocepacia* in human and mouse macrophages [20,31,32], we next compared *B. cenocepacia*-induced CASP4 expression and the activation of CASP1 in WT, *mefv*^{-/-}, and *casp4*^{-/-} macrophages at 6 h post infection via immunoblot. Expression of CASP4 in response to *B. cenocepacia* was markedly induced in WT and *mefv*^{-/-} macrophages (Fig. S2A). With respect to *B. cenocepacia*-induced CASP1 activation, proteolytic processing of CASP1 was comparably decreased in both *mefv*^{-/-} and *casp4*^{-/-} macrophages compared to the corresponding WT cells (Fig. S2B). These data indicate

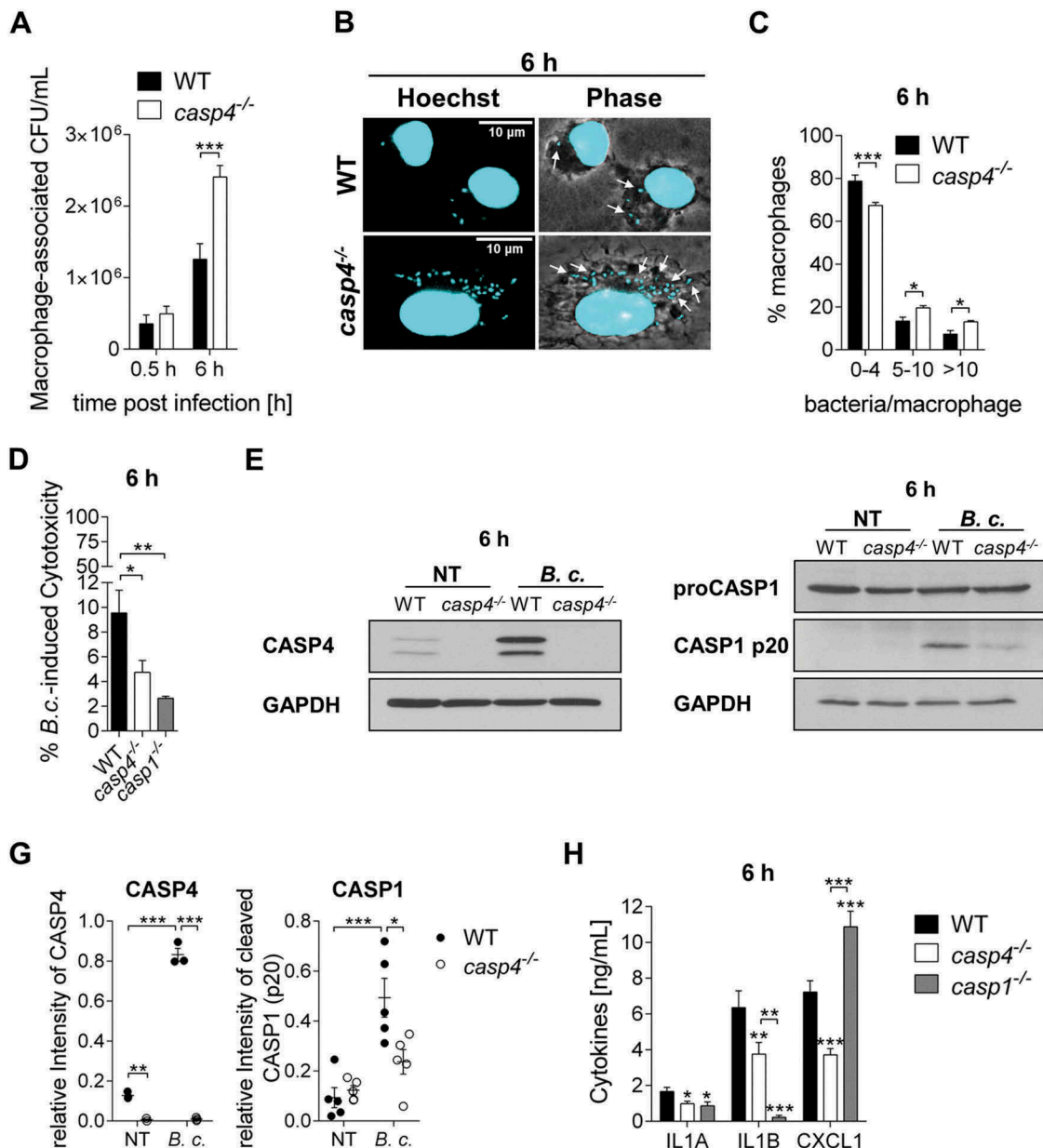


Figure 1. CASP4/caspase-11 contributes to the restriction of *B. cenocepacia* in vitro. (a) Intracellular survival of *B. cenocepacia* MH1K (*B.c.*) in WT and *casp4*^{-/-} macrophages. Data represent mean ± SEM (n = 9). Statistical analysis was performed using two-way ANOVA. (b) Immunofluorescence assay of intracellular *B. cenocepacia* in WT and *casp4*^{-/-} macrophages at 6 h post infection. White arrows point to *B. cenocepacia*. (c) Quantification of intracellular *B. cenocepacia* in WT and *casp4*^{-/-} macrophages at 6 h post infection. Values are mean percentage ± SEM calculated by scoring 60 randomly chosen fields of view from 3 experiments. Statistical analyses were performed using a linear mixed effects model. (d) *B. cenocepacia*-induced cytotoxicity was calculated by measuring LDH release in supernatants from WT and *casp4*^{-/-} macrophages at 6 h post infection. Statistical analyses were performed using one-way ANOVA. (e) Immunoblot analysis of CASP4 from WT and *casp4*^{-/-} macrophages infected with *B. cenocepacia* MH1K at 6 h post infection. (f) CASP1 immunoblot analysis of whole cell lysates from WT and *casp4*^{-/-} macrophages infected with *B. cenocepacia* MH1K at 6 h post infection. (g) Densitometry analysis of CASP4 (n = 3) and cleaved CASP1 (n = 5) at 6 h post infection. Shown are mean ± SEM. Statistical analysis was performed using two-way ANOVA. (h) Cytokine release at 6 h from WT, *casp4*^{-/-} and *casp1*^{-/-} macrophages infected with *B. cenocepacia* (n = 9). Shown are mean ± SEM. Statistical analysis was performed using one-way ANOVA. *p ≤ 0.05, **p ≤ 0.01, ***p ≤ 0.001. NT, no treatment.

that both MEFV/PYRIN and CASP4 contribute to CASP1 activation in response to *B. cenocepacia* infection.

CASP4 promotes the restriction of *B. cenocepacia* and the release of cytokines in vivo

Next, to examine if CASP4 deficiency also contributes to *B. cenocepacia* persistence in vivo, we infected WT and *casp4*^{-/-} mice intratracheally with sublethal and lethal doses of *B.*

cenocepacia and followed the course of infection. After sublethal infection, bacterial loads in *casp4*^{-/-} mice were increased by 3.5-fold in the lung and by 2.5-fold in the spleen after 48 h when compared to the corresponding WT mice (Figure 2a). We also found that lethal doses of *B. cenocepacia* led to the death of all WT mice, whereas 75% of *casp4*^{-/-} mice survived at the end of the experiment at day 8 post infection (Figure 2b). Notably, *casp4*^{-/-} mice exhibited significantly lower amounts of the inflammatory cytokines IL1A, IL1B,

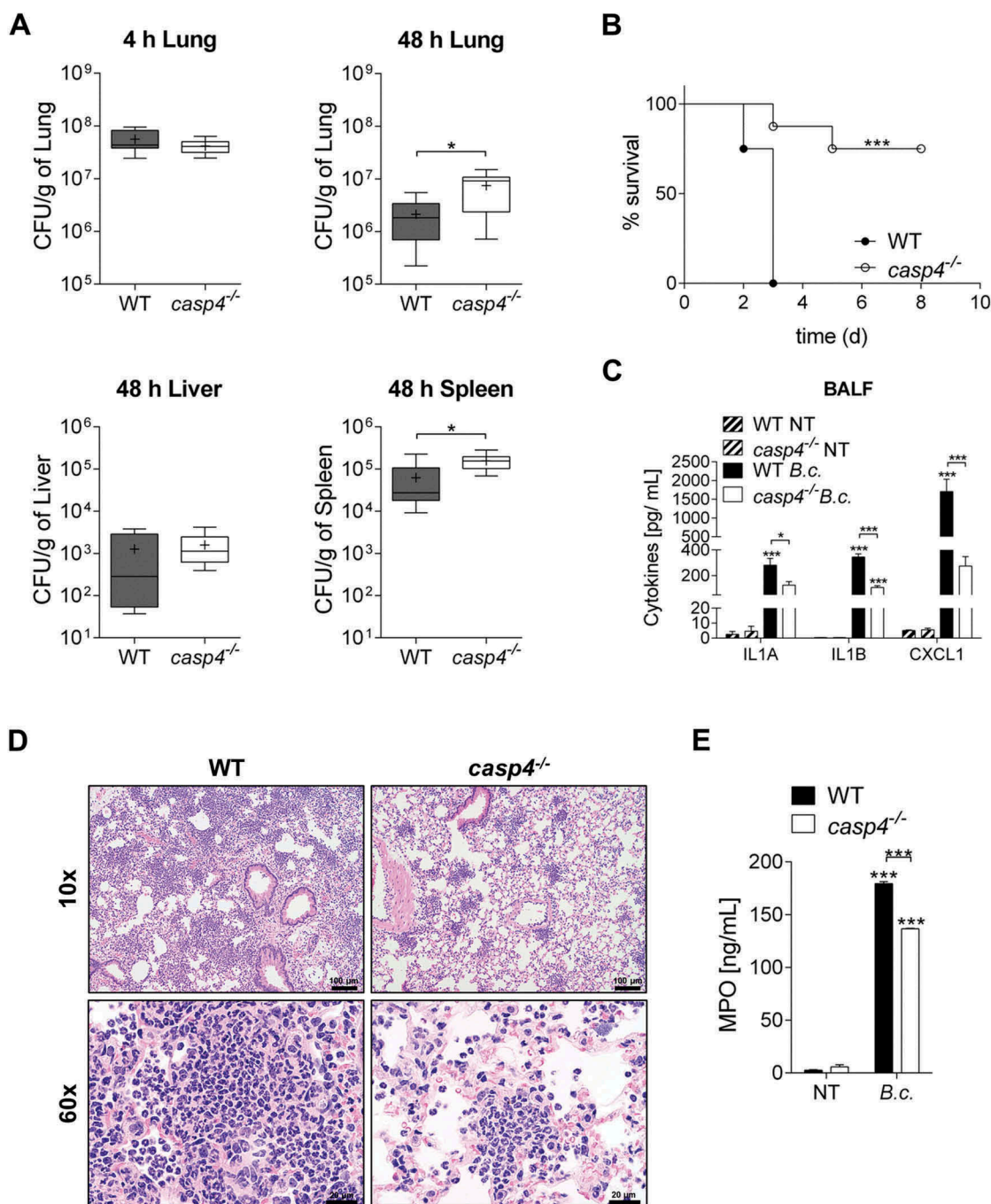


Figure 2. CASP4/caspase-11 contributes to the restriction of *B. cenocepacia* in vivo. (a) *In vivo* CFU from lung, liver and spleen of WT and *casp4*^{-/-} mice infected with *B. cenocepacia* K-56 (B.c.) at 4 h (n = 9) and 48 h (n = 10). Pooled data from 2 independent experiments are shown as mean ± SEM. Statistical analysis was performed using two-tailed Student's t-test. (b) Survival of WT and *casp4*^{-/-} mice after intratracheal infection with 30 × 10⁶ CFU. Pooled data from 2 independent experiments (n = 8). Statistical analysis was performed using Log-rank (Mantel-Cox) test. (c) Cytokine levels at 24 h in the BALF of WT (n = 7) and *casp4*^{-/-} (n = 6) mice after intratracheal infection with 30 × 10⁶ CFU. Statistical analysis was performed using two-way ANOVA. (d) Representative 10x (upper panel) and 60x (lower panel) magnification of H&E-stained lung sections from WT and *casp4*^{-/-} mice showing increased inflammatory infiltrate within the lung sections. (e) MPO levels at 24 h in the BALF of WT and *casp4*^{-/-} mice treated as in (C). Statistical analysis was performed using two-way ANOVA. *p ≤ 0.05, **p ≤ 0.01, ***p ≤ 0.001.

and CXCL1/KC in their bronchoalveolar lavage fluid (BALF) (Figure 2c) despite increased bacterial persistence in their lungs (Figure 2a). Histological sections of lung tissue from WT mice were characterized by marked alveolitis, multifocal vasculitis and fibrin exudation (Figure 2d and S3A). Compared to their *casp4*^{-/-} counterparts, WT mice showed marked to severe inflammatory cell infiltration (Figure 2d)

with increased levels of the inflammatory marker MPO (myeloperoxidase) in the BALF (Figure 2e). Notably, *B. cenocepacia* was still present in the lungs of surviving *casp4*^{-/-} mice, indicating that the mice did not clear the infection (Fig. S3B). Together, these results indicate that expression of CASP4 restricts survival and dissemination of *B. cenocepacia* during infection, yet is associated with increased inflammatory

cytokine production and the biomarker MPO, and decreased host survival.

CASP4 promotes the formation of the *B. cenocepacia*-containing autophagosome

Because functional autophagy is important to clear intracellular *B. cenocepacia* in WT macrophages and epithelial cells [5], we next determined if the interaction between *B. cenocepacia* and the cellular autophagy system is affected by the lack of CASP4. We quantified the colocalization of *B. cenocepacia* with the autophagy marker LC3 in macrophages, and found fewer colocalization events at 0.5 h and 2 h post infection in the absence of CASP4 compared to WT cells (Figure 3a and b). Because stimulation of autophagy is characterized by the formation of autophagosomes, which can be identified as puncta using confocal microscopy, we next determined if puncta are formed in *casp4*^{-/-} macrophages in response to infection. Notably, CASP4 deficiency led to reduced LC3 puncta formation in response to *B. cenocepacia* infection (Figure 3c). In contrast, no difference in LC3 colocalization between WT and *casp4*^{-/-} macrophages was detected after infection with nonpathogenic *E. coli* (Figure 3d). Accordingly, restriction of intracellular *E. coli* was comparable in WT and *casp4*^{-/-} macrophages (Fig. S4A). Therefore, these data indicate that CASP4 is required for the restriction of *B. cenocepacia* and its enclosure within autophagosomes but not for *E. coli*.

Another approach to detect the formation of autophagosomes is to determine the amount of cleavage and lipidation of LC3-I into LC3-II by western blot. To determine if *B. cenocepacia* infection was accompanied by the formation of autophagosomes, *B. cenocepacia*-induced LC3-II conversion was examined via immunoblot. The production of LC3-II upon *B. cenocepacia* infection was significantly lower within *casp4*^{-/-} macrophages compared to their WT counterparts (Figure 3e and f). In WT macrophages, autophagy was clearly induced in response to *B. cenocepacia*, whereas nonpathogenic *E. coli* did not promote LC3-II conversion (Figure 3e-h and S4D-E).

The T6SS of *B. cenocepacia* is essential for intracellular pathogenicity [19,32]. Accordingly, T6SS deficiency led to enhanced phagocytosis and the impairment of bacterial replication in WT macrophages (Fig S4B and C). In addition, *B. cenocepacia* ΔT6SS did not induce autophagy within WT or *casp4*^{-/-} macrophages. Figure 3g-h and S4F demonstrate that there was no significant increase in LC3-II formation upon infection with *B. cenocepacia* ΔT6SS when compared to non-infected control cells. To further visualize *B. cenocepacia* and its surrounding compartment in WT and *casp4*^{-/-} macrophages, we used qualitative transmission electron microscopy (TEM). As shown in Figure 3i, in WT macrophages, *B. cenocepacia* was present in a multilamellar membrane structure typical of autophagosomes, whereas bacteria were enclosed by a single membrane in *casp4*^{-/-} macrophages. Together, these results indicate that formation of autophagosomes in response to pathogenic *B. cenocepacia* is compromised in *casp4*^{-/-} macrophages and requires a functional bacterial T6SS.

The absence of CASP4 impairs the delivery of *B. cenocepacia* to the lysosome

Degradation of bacteria such as *L. pneumophila* and *B. cenocepacia* via autophagy requires the fusion of the cargo-transporting autophagosomes with lysosomal compartments, leading to the formation of autolysosomes. Yet, a possible role of CASP4 in the trafficking of autophagosomes has not been examined. To determine if CASP4 contributes to the trafficking of compartments containing *B. cenocepacia* to lysosomes, we examined the uptake of LysoTracker Green by phagosomes containing *B. cenocepacia* via confocal microscopy in WT and *casp4*^{-/-} macrophages. No difference in the number of bacteria colocalized with LysoTracker Green could be found between WT and *casp4*^{-/-} macrophages during the early stages of infection (0.5 h). However, at later time points, WT macrophages exhibited significantly more bacteria colocalized with LysoTracker Green-labeled compartments than was seen with CASP4-deficient cells (Figure 4a and b). In addition, total LysoTracker Green fluorescence was decreased at 2 h post infection in both cell types, yet more pronounced in *casp4*^{-/-} macrophages (Figure 4c). To further determine, if *B. cenocepacia* requires the T6SS to reduce acidic organelles, we compared total LysoTracker Green fluorescence in WT macrophages upon infection with *B. cenocepacia* and its corresponding T6SS mutant, or nonpathogenic *E. coli*. *B. cenocepacia* significantly reduced LysoTracker Green fluorescence in WT macrophages in a multiplicity of infection (MOI)-dependent manner (Figure 4d). In contrast, macrophages infected with *B. cenocepacia* ΔT6SS or *E. coli*, exhibited a similar level of LysoTracker Green fluorescence as measured in non-treated cells (Figure 4d). These results indicate that whereas CASP4 mediates the fusion of *B. cenocepacia*-containing compartments with lysosomes, the pathogen uses its T6SS to reduce the number of acidic compartments within macrophages.

***B. cenocepacia*-containing autophagosomes require the enzymatic activity of CASP1 and CASP4 to fuse with lysosomes**

Because CASP4 is partially required for CASP1 activity in response to *B. cenocepacia* (Figure 1f-g and S2B), we next examined if *casp1*^{-/-} macrophages display impaired trafficking of *B. cenocepacia* to acidic vesicles as well. Indeed, CASP1 deficiency decreased colocalization of *B. cenocepacia* with LysoTracker Green (Figure 4e-g). These data show that inflammasome-dependent fusion of the *B. cenocepacia*-containing vacuoles with lysosomes is mediated by both CASP4 and CASP1. To further determine if CASP1 also plays a role for the trafficking of *B. cenocepacia* to phagophores, we quantified the colocalization of *B. cenocepacia* with LC3 in WT and *casp1*^{-/-} macrophages at 0.5 h and 2 h post infection. In the absence of CASP1, fewer bacteria colocalized with LC3 (Figure 5a-c). Furthermore, to test if the enzymatic activities of CASP4 and CASP1 are required for autophagosome formation in response to *B. cenocepacia*, WT macrophages were treated with the inhibitor Ac-YVAD-CMK, which inhibits the activity of both CASP1 and CASP4. Then, the production of LC3-II was examined via immunoblot. Figure 5d-e show that

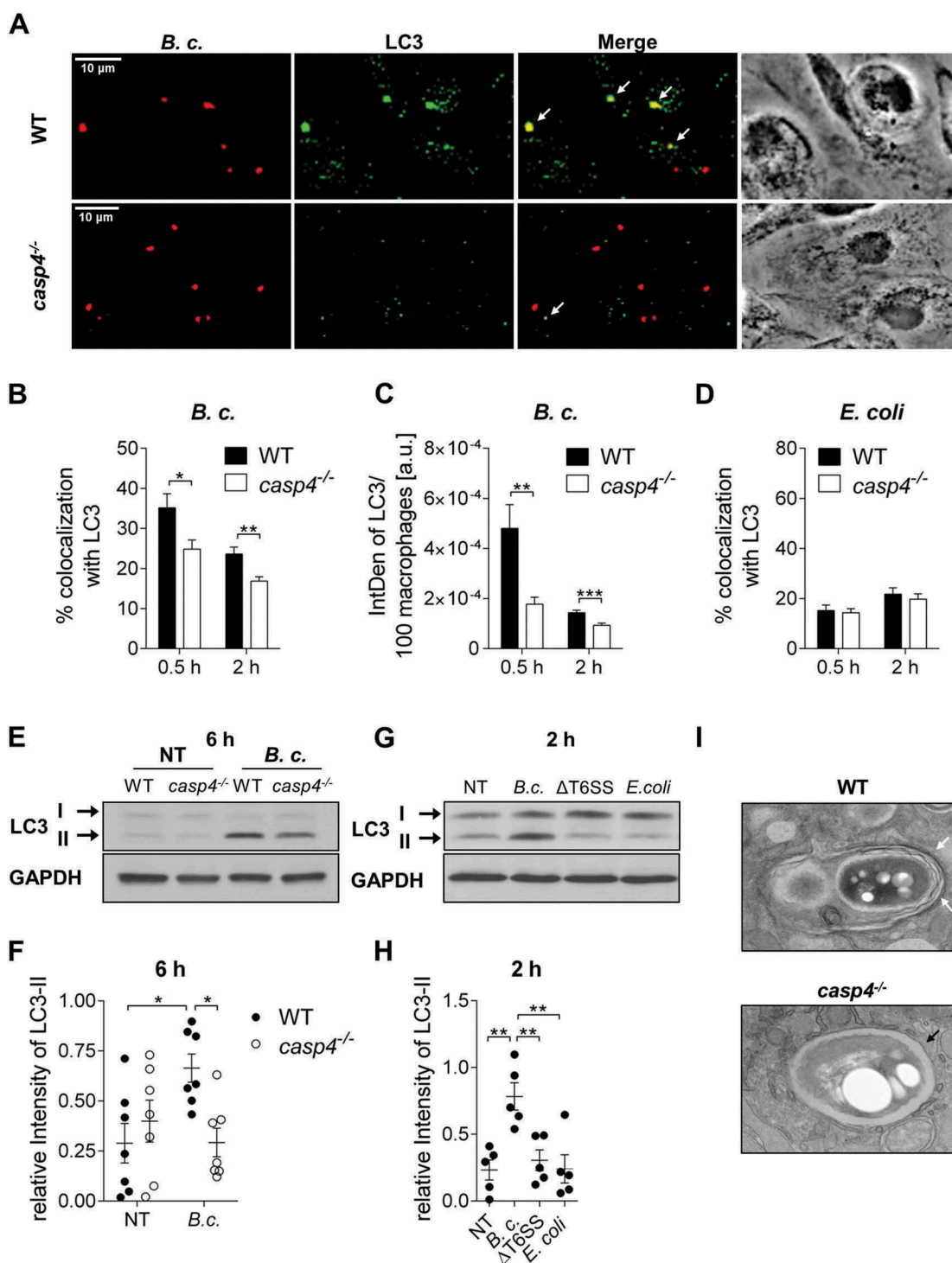


Figure 3. CASP4/caspase-11 promotes autophagosome formation in response to pathogenic bacteria. **(a)** LC3 immunofluorescence assay of *B. cenocepacia* (*B.c.*)-infected WT and *casp4*^{-/-} macrophages at 30 min post infection. White arrows point to *B. cenocepacia*-LC3 colocalization. **(b)** Quantification of *B. cenocepacia* colocalized with LC3. **(c)** Quantification of total LC3 puncta in *B. cenocepacia*-infected WT and *casp4*^{-/-} macrophages using ImageJ Software. a.u., arbitrary units. **(d)** Quantification of *E. coli* colocalized with LC3 in WT and *casp4*^{-/-} macrophages. **(A–D)** Values are mean percentage ± SEM calculated by scoring 24 randomly chosen fields of view from at least 3 experiments. Statistical analyses were performed using Student's t-test. **(e)** LC3-II immunoblot analysis from *B. cenocepacia*-infected WT and *casp4*^{-/-} macrophages at 6 h post infection. **(f)** Densitometry analysis of *B. cenocepacia*-induced LC3-II in WT and *casp4*^{-/-} macrophages at 6 h post infection. Shown are mean ± SEM of 7 independent experiments (n = 7). Statistical analysis was performed using two-way ANOVA. **(g)** LC3 immunoblot analysis in WT macrophages at 2 h after infection with *B. cenocepacia* wild-type, *B. cenocepacia* T6SS mutant and *E. coli*. **(h)** Densitometry analysis of LC3-II in WT macrophages treated as in (G). Shown are mean ± SEM of 5 independent experiments (n = 5). Statistical analysis was performed using one-way ANOVA. **(i)** Qualitative transmission electron microscopy images of *B. cenocepacia*-infected WT and *casp4*^{-/-} macrophages at 2 h post infection. White arrows indicate a multilamellar membrane characteristic for autophagosomes. Black arrow indicates a single-membrane vacuole. *p ≤ 0.05, **p ≤ 0.01, ***p ≤ 0.001. No treatment (NT).

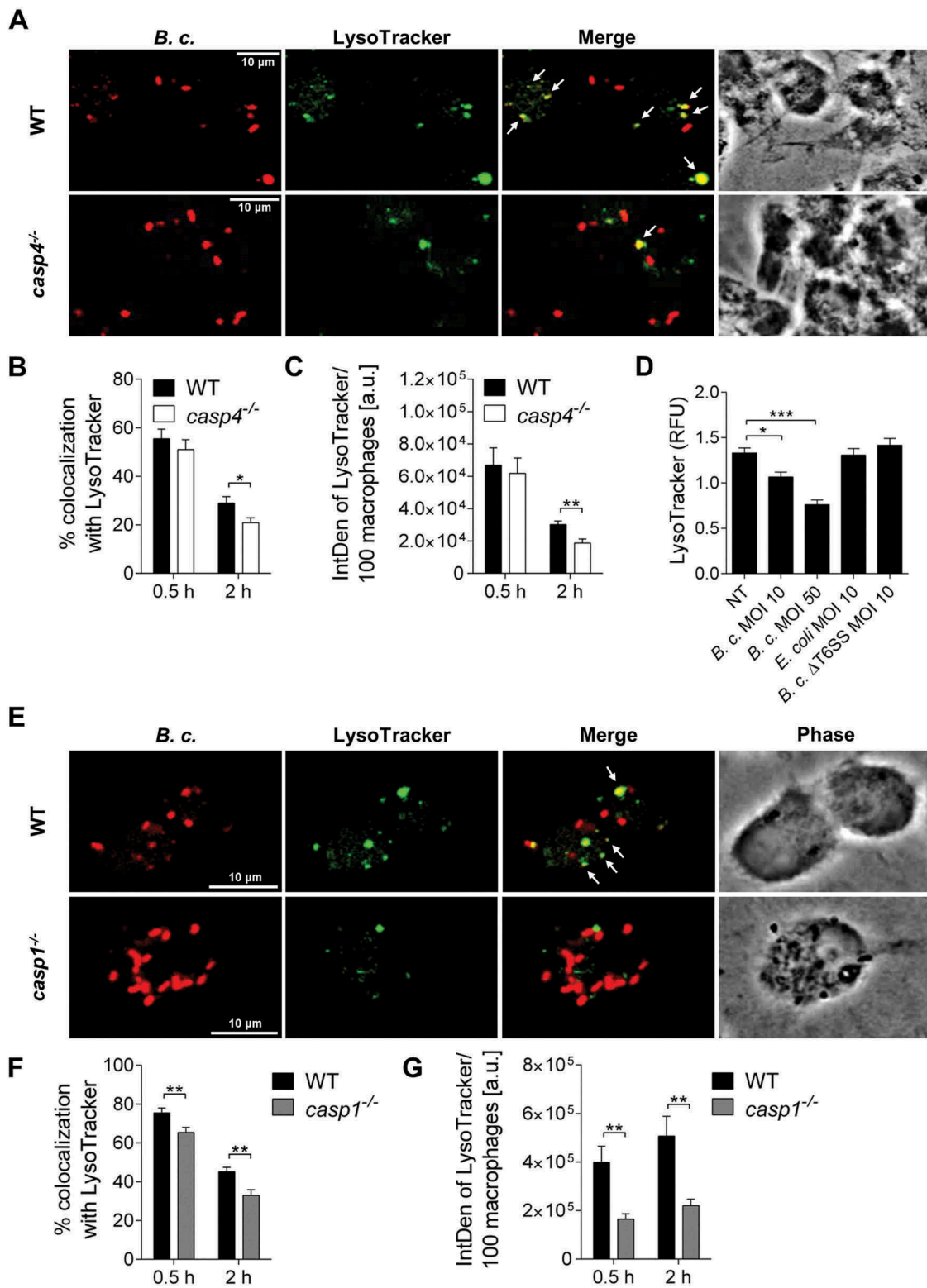


Figure 4. CASP4/caspase-11 and CASP1 modulate trafficking of the *B. cenocepacia*-containing vacuole. (a) LysoTracker Green immunofluorescence assay of *B. cenocepacia* (*B.c.*)-infected WT and *casp4*^{-/-} macrophages at 2 h post infection. White arrows point to *B. cenocepacia*-LysoTracker colocalization. (b) Quantification of *B. cenocepacia* colocalized with LysoTracker Green in WT and *casp4*^{-/-} macrophages. Statistical analyses were performed using Student's t-test. (c) Quantification of total LysoTracker Green in *B. cenocepacia*-infected WT and *casp4*^{-/-} macrophages shown in A-B using ImageJ Software. Values are mean ± SEM calculated by scoring 24 randomly chosen fields of view from at least 3 independent experiments. Statistical analyses were performed using Student's t-test. a.u., arbitrary units. (d) Total LysoTracker Green fluorescence in WT macrophages. Shown are mean ± SEM of 15 independent experiments (n = 15). Statistical analysis was performed using one-way ANOVA. (e) LysoTracker Green immunofluorescence assay of *B. cenocepacia*-infected WT and *casp1*^{-/-} macrophages at 2 h post infection. White arrows point to *B. cenocepacia*-LysoTracker colocalization. (f) Quantification of *B. cenocepacia* colocalized with LysoTracker Green WT and *casp1*^{-/-} macrophages. Statistical analyses were performed using Student's t-test. (g) Quantification of total LysoTracker Green in *B. cenocepacia*-infected WT and *casp1*^{-/-} macrophages shown in E-F using ImageJ Software. Values are mean ± SEM calculated by scoring 24 randomly chosen fields of view from at least 3 experiments. Statistical analyses were performed using Student's t-test. *p ≤ 0.05, **p ≤ 0.01, ***p ≤ 0.001. NT, no treatment.

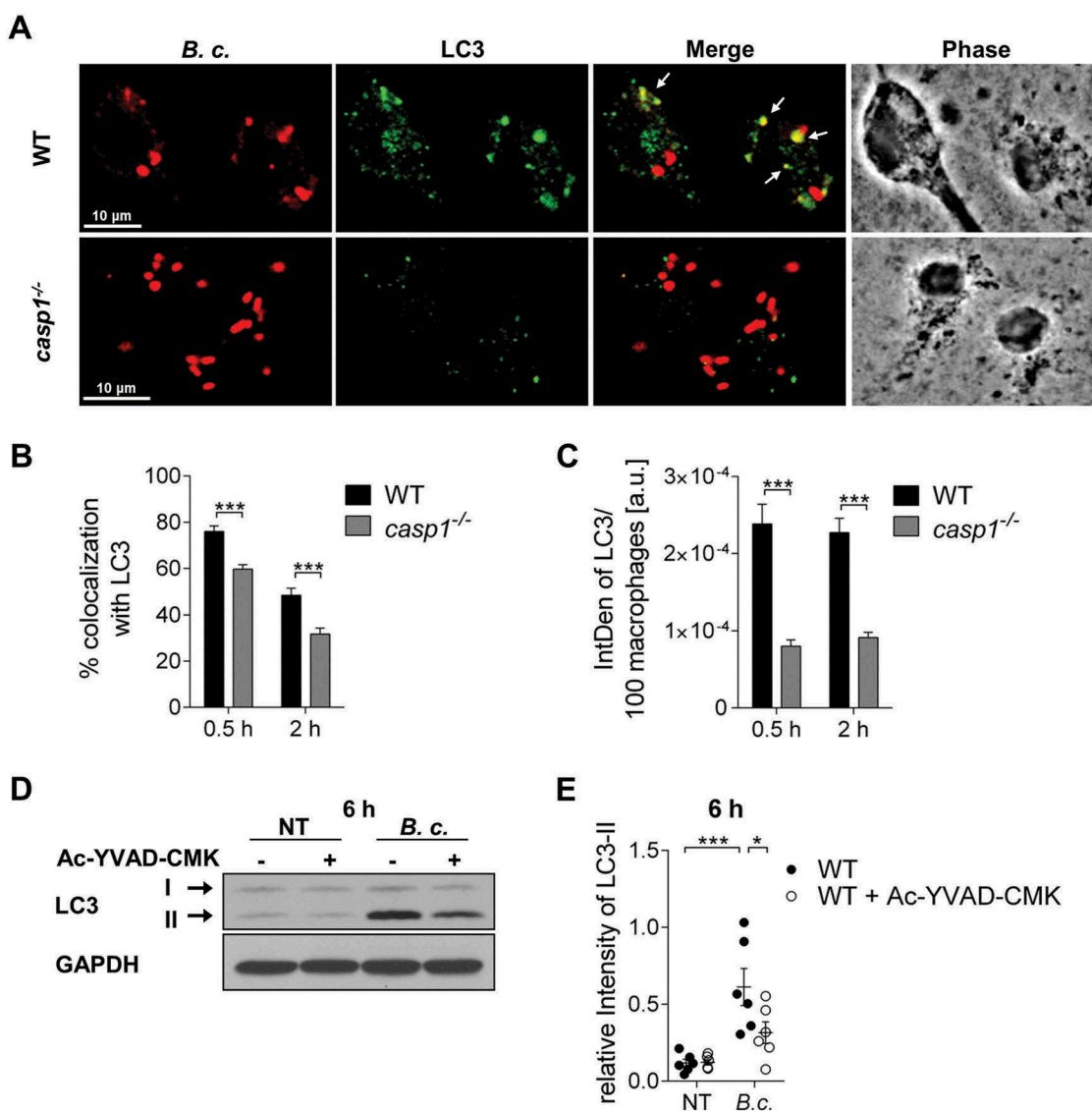


Figure 5. Autophagosome formation in response to *B. cenocepacia* requires active CASP1. (a) LC3 immunofluorescence assay of *B. cenocepacia* (*B.c.*)-infected WT and *casp1*^{-/-} macrophages at 2 h post infection. White arrows point to *B. cenocepacia*-LC3 colocalization. (b) Quantification of *B. cenocepacia* colocalized with LC3. (c) Quantification of total LC3 puncta in *B. cenocepacia*-infected WT and *casp1*^{-/-} macrophages using ImageJ Software. Values are mean percentage \pm SEM calculated by scoring 24 randomly chosen fields of view from at least 3 experiments. Statistical analyses were performed using Student's t-test. a.u., arbitrary units. (d) LC3-II immunoblot analysis from *B. cenocepacia*-infected WT macrophages treated with Ac-YVAD-CMK (50 μ M) at 6 h post infection. (e) Densitometry analysis of *B. cenocepacia*-induced LC3-II in WT macrophages treated with Ac-YVAD-CMK at 6 h post infection. Shown are mean \pm SEM of 6 independent experiments (n = 6). Statistical analysis was performed using two-way ANOVA. *p \leq 0.05, **p \leq 0.01, ***p \leq 0.001. NT, no treatment.

Ac-YVAD-CMK treatment reduced the production of LC3-II at 6 h post infection. Thus, the autophagy response to *B. cenocepacia* requires enzymatically active CASP1 and CASP4.

CASP4 deficiency is accompanied by the accumulation of RAB7 during *B. cenocepacia* infection

RAB proteins are small GTPases that, when activated in their GTP-bound form, regulate vesicle trafficking and fusion events. RAB7, usually present on late endosomes, regulates the transport of endocytic membranes [33,34], and promotes the maturation of autophagic compartments [35]. To determine the mechanism by which CASP4 mediates *B. cenocepacia*-phagosome maturation, we examined if the recruitment of

RAB7 to the *B. cenocepacia*-containing vacuoles is altered in *casp4*^{-/-} macrophages. Notably, there was increased colocalization of *B. cenocepacia* with RAB7 (Figure 6a-b) accompanied by an accumulation of RAB7-positive compartments in the absence of CASP4 (Figure 6c). An increase in RAB7 expression in *casp4*^{-/-} macrophages after infection with *B. cenocepacia* was also observed by immunoblotting (Figure 6d-e). Interestingly, RAB7 activity assessed by immunoprecipitation of the GTP bound form revealed a higher proportion of GTP-bound RAB7 in *B. cenocepacia*-infected *casp4*^{-/-} macrophages compared to the corresponding WT cells (Figure 6f-g). Thus, CASP4 deficiency is characterized by an accumulation of RAB7 around the *B. cenocepacia*-containing vacuole.

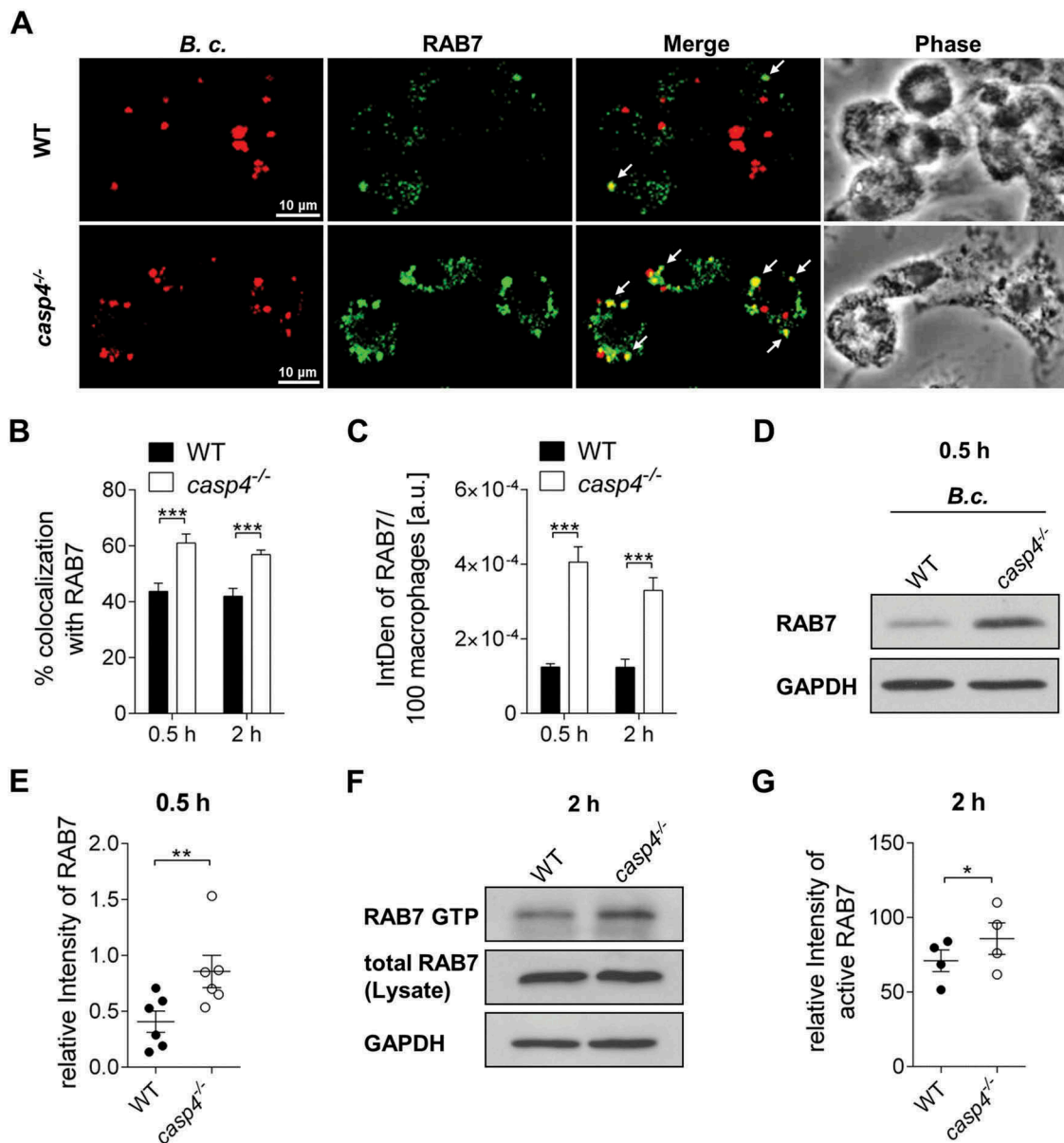


Figure 6. *casp4*^{-/-}/*caspase-11*^{-/-} macrophages accumulate RAB7 around the *B. cenocepacia*-containing vacuole. (a) RAB7 immunofluorescence assay of *B. cenocepacia* (*B.c.*)-infected WT and *casp4*^{-/-} macrophages at 30 min post infection. White arrows point to *B. cenocepacia*-RAB7 colocalization. (b) Quantification of *B. cenocepacia* colocalized with RAB7. (c) Quantification of RAB7 in *B. cenocepacia*-infected WT and *casp4*^{-/-} macrophages using ImageJ Software. (A-C) Values are mean percentage \pm SEM calculated by scoring 24 randomly chosen fields of view from at least 3 experiments. Statistical analyses were performed using Student's t-test. a.u., arbitrary units. (d) RAB7 immunoblot analysis from WT and *casp4*^{-/-} macrophages infected with *B. cenocepacia* at 30 min post infection. (e) Densitometry analysis of RAB7 in *B. cenocepacia*-infected WT and *casp4*^{-/-} macrophages. Shown are mean \pm SEM of 6 independent experiments (n = 6). Statistical analyses were performed using paired t-test. (f) Immunoprecipitation of GTP-bound RAB7 in *B. cenocepacia*-infected WT and *casp4*^{-/-} macrophages at 2 h post infection. (g) Densitometry analysis of active RAB7 in *B. cenocepacia*-infected WT and *casp4*^{-/-} macrophages. Shown are mean \pm SEM of 4 independent experiments (n = 4). Statistical analyses were performed using paired t-test. * $p \leq 0.05$, ** $p \leq 0.01$, *** $p \leq 0.001$.

Less *B. cenocepacia*-containing vacuoles associate with CFL1 (cofilin 1, non-muscle) in *casp4*^{-/-} macrophages

Microtubules and actin filaments provide a scaffold to allow vesicular trafficking, and remodeling of the actin cytoskeleton involves CASP4 [16,25,36]. Depolymerization of actin filaments specifically inhibits starvation-induced autophagosome formation, indicating a critical role for actin during the early stages of autophagy [37]. The actin-binding protein CFL1 (cofilin 1, non-muscle) is a key molecule that modulates actin-remodeling. To investigate the effect of CASP4 on

CFL1 during *B. cenocepacia* infection and whether it is affected by CASP4, we followed the distribution of CFL1 in relation to the *B. cenocepacia*-containing vacuoles. Using confocal microscopy, we found that CFL1 was localized in proximity to phagosomes containing *B. cenocepacia* in WT macrophages (Figure 7a). Notably, colocalization of *B. cenocepacia* with CFL1 was reduced in the absence of CASP4 (Figure 7b). However, with regard to phagosomes harboring nonpathogenic *E. coli*, there was no difference in colocalization between WT and *casp4*^{-/-} macrophages (Figure 7c).

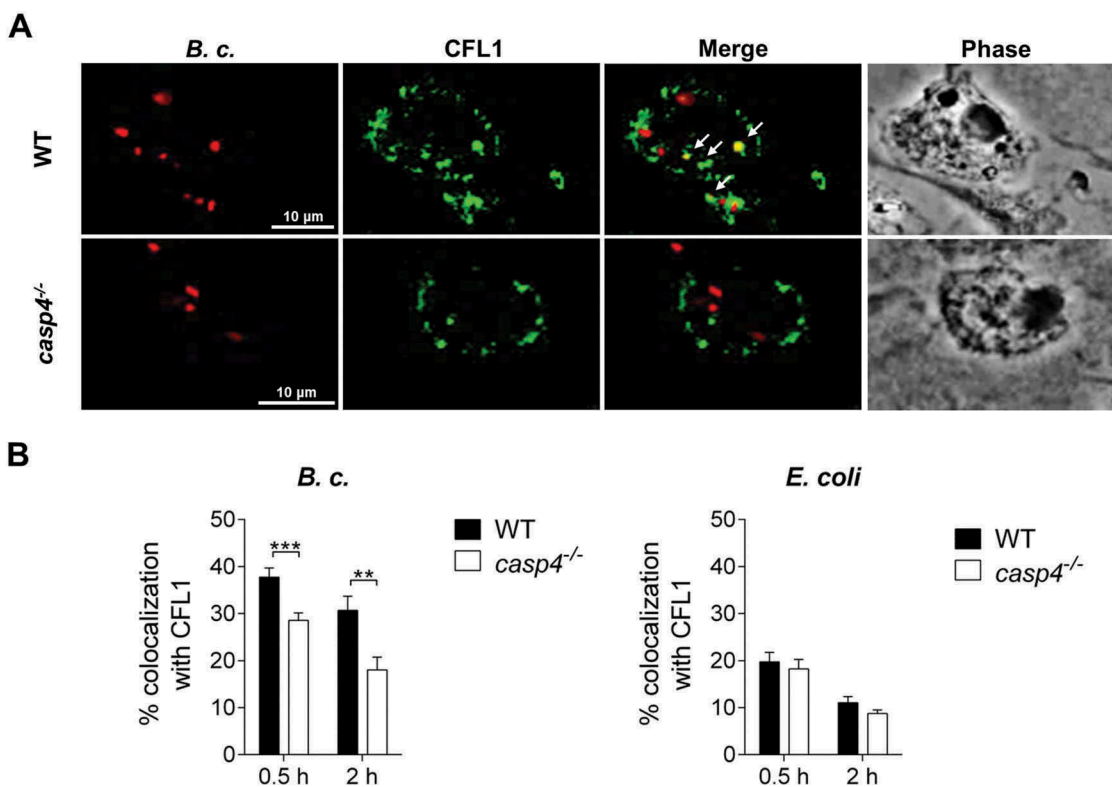


Figure 7. CFL1 associates with the *B. cenocepacia*-containing phagosome. (a) CFL1 immunofluorescence assay of *B. cenocepacia* (*B.c.*)-infected WT and *casp4*^{-/-} macrophages at 30 min post infection. White arrows point to *B. cenocepacia*-CFL1 colocalization. (b) Quantification of *B. cenocepacia* and *E. coli* colocalized with CFL1 in WT and *casp4*^{-/-} macrophages. Values are mean percentage \pm SEM calculated by scoring 24 randomly chosen fields of view from at least 3 experiments. Statistical analyses were performed using Student's t-test. ** $p \leq 0.01$, *** $p \leq 0.001$.

Together, these results indicate that CASP4 affects the recruitment of CFL1 in response to *B. cenocepacia* infection.

Discussion

Our study shows that CASP4 promotes the restriction of *B. cenocepacia* *in vitro* and *in vivo*. Although, CASP4 has been implicated in the restriction of *L. pneumophila* and the closely related *Burkholderia* species *B. pseudomallei* and *B. thailandensis*, the exact mechanism is still unclear [16,38]. Recognition of intracellular *B. cenocepacia* in murine macrophages is mediated through NOD-like receptors including NLRP3 and MEFV/PYRIN [19,20]. Non-canonical NLRP3-PYCARD/ASC-dependent inflammasome activation in response to Gram-negative pathogens requires CASP4 [15]. Here, we report that both CASP4 and MEFV/PYRIN are required for *B. cenocepacia*-induced CASP1 activation. Accordingly, cleavage of CASP7 downstream of CASP1 was also diminished in the absence of CASP4. Cleaved CASP7, as a result of CASP1 activation, has been described for *S. Typhimurium* [29], *L. pneumophila* [30] and *B. pseudomallei* [39] infection, all of which are pathogens predominantly sensed by the NLRC4 inflammasome [16]. Thus, our results demonstrate that CASP1-dependent CASP7 activation is not restricted to the NLRC4 inflammasome. Inflammasome activation via MEFV/PYRIN might very well account for the residual CASP7 activation observed in our study. However, putative CASP7 activity downstream of MEFV/PYRIN has yet to be determined.

The lack of CASP4, rather than CASP1, protects against lipopolysaccharide-induced septic shock due to reduced secretion of the pro-inflammatory cytokines IL1A and IL1B [15,40]. Yet, *casp4*^{-/-} mice are highly susceptible to infection with virulent *B. pseudomallei* and avirulent *B. thailandensis* resulting in increased mortality [18]. In contrast, in our present study, we report for the first time that CASP4 deficiency mediates resistance to a lethal dose of *B. cenocepacia* even though *casp4*^{-/-} mice showed that bacteria persisted within the lung at 8 days post infection. Notably, despite an increased pulmonary burden of *B. cenocepacia*, *casp4*^{-/-} mice produced less IL1A and IL1B compared to WT in their BALF. In addition, we found reduced levels of the chemokine CXCL1/KC in the BALF of *B. cenocepacia*-infected *casp4*^{-/-} mice, which could account for the reduced inflammatory infiltrate observed in these animals. In support of these findings, the levels of IL1A, IL1B, and CXCL1/KC released by *casp4*^{-/-} macrophages were significantly reduced *in vitro* compared to WT cells. In this context, it should be noted, that mice deficient in MEFV/PYRIN exhibit reduced lung inflammation in response to *B. cenocepacia* infection as well [31]. Furthermore, *mefv*^{-/-} macrophages stimulated with *B. cenocepacia* are characterized by decreased CASP1 activation and IL1B production [31], suggesting a possible link or cooperation between CASP4 and MEFV/PYRIN that orchestrates inflammation during *B. cenocepacia* infection.

The transcription of genes coding for major autophagy proteins is downregulated upon *B. cenocepacia* infection in both WT and CFTRΔF508 (CF) macrophages, suggesting that *B. cenocepacia* actively interferes with the autophagy pathway [5]. Nevertheless, WT macrophages successfully restrict *B. cenocepacia* growth, as functional autophagy machinery is restored in WT but not in CF cells [5,41]. Reduced autophagy activity has been implicated in dysfunctional cellular immunity to intracellular pathogens including the bacteria *L. pneumophila*, *M. tuberculosis*, *L. monocytogenes*, and parasites including *Toxoplasma gondii* [7,42,43].

Because colocalization of *B. cenocepacia* with lysosomes is reduced in *casp4*^{-/-} macrophages, this raises the question of whether CASP4 takes part in the formation and maturation of autophagosomes. Here, we demonstrate that *casp4*^{-/-} macrophages exhibit less LC3-stained autophagosomes (puncta) upon *B. cenocepacia* infection compared to WT cells, suggesting that CASP4 contributes to the autophagic response against bacterial pathogens (xenophagy). In fact, inflammasome components play a role in autophagosome formation [23]. Accordingly, inflammatory CASP1 has been described to coordinate autophagy in response to *L. pneumophila* [24]. However, this is the first report of CASP4 deficiency negatively affecting autophagy in macrophages, which may explain the ability of other autophagy-interacting bacteria to be cleared in the presence of CASP4 [2,8,16]. In contrast, clearance of nonpathogenic *E. coli* does not depend on CASP1 or CASP4 [16,25]. Notably, *B. cenocepacia* lacking a functional T6SS fails to induce autophagy in macrophages. This finding is corroborated by other reports demonstrating that *P. aeruginosa* and *V. parahaemolyticus* T6SS contribute to the activation of autophagy [44,45].

In addition, we found that *casp4*^{-/-} macrophages infected with *B. cenocepacia* exhibit increased levels of total RAB7 and active GTP-bound RAB7, indicating that RAB7 activity is differentially modulated in the absence of CASP4. RAB7 has been implicated in lysosome biogenesis [46] and controls the interaction and fusion of late endosomes with lysosomes [47]. Active GTP-bound RAB7 on the surface of phagosomes promotes membrane motility leading to phagolysosome formation [26]. In addition, RAB7 regulates the final maturation of late autophagic vacuoles during starvation-induced autophagy [48]. Interestingly, *B. cenocepacia* inactivates RAB7 [12]. Because active RAB7 accumulates in *casp4*^{-/-} macrophages, these data suggest that the inactivation of RAB7 by *B. cenocepacia* requires CASP4. Yet, it is also plausible to hypothesize that RAB7 accumulation on the *B. cenocepacia*-containing vacuoles is a result rather than a cause of arrested maturation. Recent reports demonstrate that RAB7 interacts with ATG4B, a key cysteine protease that cleaves LC3, and hence RAB7 seems to act as a negative regulator of autophagy which corroborates our findings in *casp4*^{-/-} macrophages [49].

Likewise, the absence of PIK3C3/VPS34 which plays a crucial role in autophagosome formation and autophagic flux is characterized by RAB7 hyperactivation [50–52]. PIK3C3/VPS34 deficiency prevents recruitment of TBC1D2/Armus (the RAB7-specific GTPase activation protein) to

endosomal membranes. TBC1D2 interacts with LC3 and regulates RAB7-GTP hydrolysis selectively on autophagosomes to enable fusion with lysosomes and subsequent degradation of the transported cargo [53]. Thus, higher amounts of RAB7-GTP in *B. cenocepacia*-infected *casp4*^{-/-} macrophages may be attributed to decreased GTPase activity around the *B. cenocepacia*-containing vacuoles.

RAB7 on the surface of phagosomes was further reported to promote membrane motility leading to phagolysosome formation via recruitment of the effector protein RILP, which mediates the contact of phagosomes with microtubule-associated motor proteins [26]. Microtubules organize the formation of autophagosomes, their transport, and subsequent fusion events [54–56] by electrostatic interactions originating from the N-terminal domain of LC3 thereby allowing the attachment of autophagosomes to the microtubule network [57,58]. Chemical disruption of microtubules reduces the formation of mature autophagosomes [55]. Concurrently, actin-depolymerizing agents, such as latrunculin B or cytochalasins, reduce starvation-induced autophagosome formation without affecting general acidification of the autophagosome [37,59]. Nonetheless, details about the role of actin during autophagy of bacteria (xenophagy) are limited.

Here, we propose a role for CASP4 in autophagy through the modulation of actin dynamics during bacterial infection. CASP4 facilitates cell migration by directly interacting with the actin interacting protein WDR1/AIP1, thereby allowing CFL1-dependent actin depolymerization in the context of chemotaxis [36]. During phagocytosis, F-actin assembly around phagosomes is crucial to guarantee efficient phagosome-lysosome fusion [60]. However, the role of CASP4-actin interaction in intracellular autophagosome trafficking is still unclear. Notably, CASP4-dependent degradation of *L. pneumophila* in restrictive macrophages is driven by F-actin polymerization around the periphery of the *L. pneumophila*-containing vacuole. Likewise, we found reduced amounts of CFL1 adjacent to the *B. cenocepacia*-containing vacuole in CASP4-deficient cells. *casp4*^{-/-} macrophages also exhibit significantly lower amounts of active RHOA and inactive CFL1, even under basal conditions [25]. In addition, the *B. cenocepacia* T6SS effector TecA mediates the deamidation of RHOA in murine cells [32]. RHOA is well known for its ability to induce actin-derived stress fibers and focal adhesions [61], and it also promotes the activation of LIM kinases, which inhibit CFL1 via phosphorylation [62,63].

Compartments in WT macrophages harboring *L. pneumophila* or *B. cenocepacia* have the characteristics of autophagosomes and proceed to fuse with lysosomes. However, in permissive *casp4*^{-/-} and *casp1*^{-/-} cells, the recruitment of lysosomes to vacuoles containing these pathogens is decreased. Notably, the number of lysosomes is reduced in *casp4*^{-/-} and *casp1*^{-/-} macrophages. Together, it is plausible to conclude that dysfunctional regulation of actin dynamics via CFL1 in the absence of CASP4 compromises the formation and trafficking of autophagosomes leading to accumulation of RAB7 during bacterial infection. In summary, our data present an intricate and novel relation between inflammatory caspases and the autophagy machinery.

Materials and methods

Bacterial strains

B. cenocepacia K56–2 is a clinical isolate obtained from a CF patient. Its derivative MH1K is a gentamicin-sensitive strain [64]. *B. cenocepacia* K56–2 or nonpathogenic *E. coli* BL21 used in immunofluorescence experiments are transformed with a plasmid for red fluorescent protein (Ds-Red). *B. cenocepacia* ΔT6SS was kindly provided by Dr. Valvano at Queen's University, Belfast, UK. All bacterial strains were grown overnight in LB medium at 37°C and 200 rpm as previously described [5,14,41,65].

Mice

C57BL/6 WT mice were obtained from The Jackson Laboratory (Bar Harbor, ME, USA). *casp4*^{-/-}/*caspase-11*^{-/-} mice were generously provided by Dr. Junying Yuan (Harvard Medical School, Boston, MA, USA) [40]. *casp1*^{-/-} *Casp4/Casp-11*Tg mice were a gift from Dr. Vishva Dixit (Genentech) [15]. *mefv*^{-/-}/*Pyrin*^{-/-} mice were a generous gift from Dr. Thirumala -Devi Kanneganti (St. Jude Children's Research Hospital). All mice are in the C57BL/6 background. All mice were housed in a pathogen-free facility and experiments were conducted with approval from the Animal Care and Use Committee at The Ohio State University (Columbus, OH, USA).

In vivo infection

For intratracheal infection, mice were anesthetized with Isoflurane and inoculated with 100 μl of phosphate-buffered saline (PBS; Thermo Fisher Scientific, 14,190,144) containing 10 × 10⁶ (organ CFU, histology) or 30 × 10⁶ (survival study) bacteria. To determine the bacterial load in organs, mice were sacrificed at 4 h and 24 h post infection to collect lung, liver and spleen for homogenization in PBS as previously described [5,16]. Data are presented as CFU per gram of organ. For survival experiments, animals were monitored daily for 8 days in total.

Bone marrow-derived macrophages

For the generation of primary bone marrow-derived macrophages from mice, tibias and femurs were flushed with IMDM medium (Thermo Fisher Scientific, 12,440,053) supplemented with 10% fetal bovine serum (Thermo Fisher Scientific, 16,000,044), 50% L cell-conditioned medium [66,67], 0.6x MEM non-essential amino acids (Thermo Fisher Scientific, 11,140,050) and 0.1% penicillin and streptomycin (Thermo Fisher Scientific, 15,140,122) as previously described [5,16,25,30,41,65]. Cells were cultivated at least 6 days at 37°C in a humidified atmosphere containing 5% CO₂.

Cell culture and infection of primary macrophages

Prior to experiments, macrophages were cultivated in IMDM medium supplemented with 10% fetal bovine serum for at least 1 h. To stimulate autophagy, cells were incubated with 5 μg/mL rapamycin (Sigma Aldrich, R0395) 1 h prior to

infection and continuously until the end of the experiment. To inhibit CASP1 and CASP4/caspase-11 activity, macrophages were incubated with 50 μM Ac-YVAD-CMK (Enzo Life Sciences, ALX-260–028) 1 h prior to infection and continuously until the end of the experiment. *In vitro* infections were performed with an MOI 10:1, including centrifugation for 5 min at 30xg to synchronize the infection. To determine cleavage of CASP1 via immunoblotting, macrophages were treated with an MOI 50:1. To analyze intracellular bacterial replication in WT and *casp4*^{-/-} macrophages, cells were infected with *B. cenocepacia* MH1K for 1 h followed by 30 min incubation with 50 μg/mL gentamicin (Thermo Fisher Scientific, 15,750–060) to avoid extracellular bacterial replication. In contrast, to determine intracellular CFUs of the gentamicin-resistant *B. cenocepacia* T6SS mutant strain, macrophages were extensively washed 3x with PBS after the initial infection for 1 h. At the indicated time points, macrophages were lysed using 0.1% Triton X-100 (Fisher Scientific, BP151) in PBS, and serial dilutions of the lysates were incubated on LB agar for 48 h.

Confocal microscopy

Macrophages were cultured on glass coverslips in 24-well plates and fixed with 4% paraformaldehyde for 30 min at the indicated time points. For permeabilization, cells were treated with ice cold methanol for 10 sec (LC3, CFL1) or 0.1% Triton X-100 for 20 min (RAB7) followed by blocking with 5% goat serum (Thermo Fisher Scientific, 16,210,064) in PBS. LC3A/B (Cell Signaling Technology, 4108), CFL1 (Cell Signaling Technology, 5175), and RAB7 (Cell Signaling Technology, 9367,) were visualized using goat anti-rabbit IgG secondary antibody conjugated to Alexa Fluor® 488 (Molecular Probes, A-11,008,). LysoTracker™ Green (Molecular Probes, L7526) was used to stain acidic compartments of infected macrophages. Nuclei were stained with 1 μg/mL 4',6'-diamino-2-phenylindole (DAPI; Molecular Probes, D1306,) in PBS-5% goat serum for 5 min. To stain intracellular *B. cenocepacia* strain MH1K, live macrophages were incubated with 1 μg/mL Hoechst in PBS for 20 min and subsequently fixed with 4% paraformaldehyde. Images were captured using a laser scanning confocal fluorescence microscope with a 60X objective (Olympus Fluoview FV10i) as previously described [25,41,65]. Intensities of target proteins were measured using ImageJ Software. Graphs depict integrated density (IntDen), which is defined as the 'product of area and Mean Gray Value' of the pixel values in the selected area, normalized to the cell number.

Quantification of lysotracker green using a microplate reader

Macrophages were cultured in flat clear bottom black 96-well plates (Corning, 3603). LysoTracker Green (1 μM) and 1 μg/mL Hoechst dye were added to the cells 1 h before the measurement. Then, cells were washed 1x with PBS and growth media was replaced with Hanks balanced salt solution (Corning, 21–022-CV). Fluorescence was read using a

SpectraMax i3x microplate reader at 480/511 nm (LysoTracker Green) and 361/497 nm (Hoechst). Hoechst fluorescence was used to normalize LysoTracker Green signals.

Cytokine and MPO analysis

Cytokines in BALF were measured by the Analytical & Development Lab within the Center for Clinical and Translational Science (CCTS) at The Ohio State University using the V-PLEX Proinflammatory Panel 1 (mouse) Kit (MSD, K15048G) according to the manufacturer's instructions. MPO levels in BALF were measured using a mouse MPO ELISA kit (Hycult Biotech, HK210).

Histological analysis

Lungs were removed from infected mice, inflated with PBS and fixed in 10% formalin at room temperature. Sample preparation, processing, hematoxylin & eosin staining, and semi-quantitative slide evaluation using ordinal grading scales was performed by the Histology laboratory within the Department of Veterinary Biosciences at The Ohio State University as previously described [5].

Immunoblotting

Protein extraction from macrophages was performed using TRIzol reagent (Thermo Fisher Scientific, 15,596,026) according to the manufacturer's instructions. Briefly, after phase separation using chloroform, 100% ethanol was added to the interphase/phenol-chloroform layer to precipitate genomic DNA. Subsequently, the phenol-ethanol supernatant was mixed with isopropanol to isolate proteins. The Bradford method was used to determine protein concentrations. Equal amounts of protein were separated by 13.5% SDS-PAGE and transferred to a polyvinylidene fluoride (PVDF) membrane. Membranes were incubated overnight with antibodies against CASP4 (Sigma Aldrich, C1354), CASP1 (Genentech), cleaved CASP7 (Cell Signaling Technology, 9491), LC3 (Sigma Aldrich, L8918), RAB7 (Cell Signaling Technology, 9367), p-CFL1 (Cell Signaling Technology, 3313), CFL1 (Cell Signaling Technology, 5175) and GAPDH (Cell Signaling Technology, 2118). Corresponding secondary antibodies conjugated with horseradish peroxidase (Cell Signaling Technology, 7074; Santa Cruz Biotechnology, sc-2006) and in combination with enhanced chemiluminescence reagent (Amersham, RPN2209) were used to visualize protein bands. Densitometry analyses were performed by normalizing target protein bands to their respective loading control (GAPDH) using ImageJ software as previously described [16,25,41]. For CASP4, graphs display average values of the upper and lower band.

Immunoprecipitation of RAB7

GTP-bound RAB7 from WT and *casp4*^{-/-} macrophages was immunoprecipitated using the RAB7 Activation Assay Kit (New East Biosciences, 82,501) according to the manufacturer's instructions.

Transmission electron microscopy

Macrophages were cultured in 2-well Permanox Lab-Tek chamber slides (Nunc, 177,429) and fixed with 2.5% glutaraldehyde (Ted Pella, 18,426) in 0.1 M phosphate buffer, pH 7.4 (Fisher Scientific, S369 and S373) containing 0.1 M sucrose (Fisher Scientific, S2-500). Sample processing was performed by the Campus Microscopy & Imaging Facility at The Ohio State University as previously described [5]. Images were taken using a FEI Tecnai G2 Spirit transmission electron microscope plus AMT camera system.

Statistical analyses

Data were analyzed using GraphPad Prism 6.0 and SAS 9.4. All figures display mean and standard error of the mean (SEM) from at least 3 independent experiments as indicated in the figure legends. Comparisons between groups were conducted with Student's t-test, one-way or two-way ANOVA, or linear mixed effects model (depending on the data structure) followed by Holm's adjustment for multiple comparisons as indicated. Adjusted p-values < 0.05 were considered statistically significant.

Abbreviations

BALF	bronchoalveolar lavage fluid
BCV	<i>Burkholderia cenocepacia</i> -containing vacuole
CASP1	caspase 1
CASP4/caspase-11	caspase 4, apoptosis-related cysteine peptidase
CASP7	caspase 7
CF	cystic fibrosis
CFL1	cofilin 1, non-muscle
CFU	colony-forming unit
MAP1LC3/LC3	microtubule-associated protein 1 light chain 3
<i>Mefv/Pyrin</i>	Mediterranean fever
MPO	myeloperoxidase
RAB7	RAB7, member RAS oncogene family
T6SS	type six secretion system
WT	wild-type

Acknowledgments

We thank M. Valvano at Queen's University, Belfast, UK for providing red fluorescent *B. cenocepacia* and *B. cenocepacia* ΔT6SS strains. We thank Daniel M. Layman, Mohamed Quteifan, and Anup Vaidya for technical help. We are grateful to Dr. Sue E. Knoblaugh at the College of Veterinary Medicine/Department of Veterinary Biosciences at the Ohio State University, Columbus OH, USA for the histological evaluation of lung tissue. Comparative Pathology & Mouse Phenotyping Shared Resource, Department of Veterinary Biosciences and the Comprehensive Cancer Center, The Ohio State University, are supported in part by grant P30 CA016058. Studies in the Amer laboratory are supported by Ohio State University (OSU) Bridge funds, Public Health Preparedness for Infectious Diseases (PHPID), Center for Clinical and Translational Science (CCTS), R21 AI113477, R01 AI24121, and R01 HL127651-01A1. Cytokine analysis using the V-PLEX Proinflammatory Panel 1 (mouse) Kit was supported by Award Number Grant UL1TR001070 from the National Center For Advancing Translational Sciences. The content is solely the responsibility of the authors and does not necessarily represent the official views of the National Center For Advancing Translational Sciences or the National Institutes of Health. KK is supported by Deutsche Forschungsgemeinschaft (DFG - German Research Foundation). KC is supported by a Cystic Fibrosis Foundation Postdoctoral Research

Fellowship. AB is supported by funding from the Egyptian Government. The authors declare that they have no conflict of interests.

Disclosure statement

No potential conflict of interest was reported by the authors.

Funding

This work was supported by the | NIH | National Institute of Allergy and Infectious Diseases (NIAID) [R01AI24121];HHS | NIH | National Institute of Allergy and Infectious Diseases (NIAID) [R21AI113477]; | NIH | National Heart, Lung, and Blood Institute (NHLBI) [R01HL127651-01A1]

References

- [1] Gutierrez MG, Master SS, Singh SB, et al. Autophagy is a defense mechanism inhibiting BCG and Mycobacterium tuberculosis survival in infected macrophages. *Cell*. 2004;119(6):753–766.
- [2] Birmingham CL, Smith AC, Bakowski MA, et al. Autophagy controls Salmonella infection in response to damage to the Salmonella-containing vacuole. *J Biol Chem*. 2006;281(16):11374–11383.
- [3] Amer AO, Swanson MS. Autophagy is an immediate macrophage response to Legionella pneumophila. *Cell Microbiol*. 2005;7(6):765–778.
- [4] Nakagawa I, Amano A, Mizushima N, et al. Autophagy defends cells against invading group A Streptococcus. *Science*. 2004;306(5698):1037–1040.
- [5] Abdulrahman BA, Khweek AA, Akhter A, et al. Autophagy stimulation by rapamycin suppresses lung inflammation and infection by Burkholderia cenocepacia in a model of cystic fibrosis. *Autophagy*. 2011;7(11):1359–1370.
- [6] Rich KA, Burkett C, Webster P. Cytoplasmic bacteria can be targets for autophagy. *Cell Microbiol*. 2003;5(7):455–468.
- [7] Py BF, Lipinski MM, Yuan J. Autophagy limits Listeria monocytogenes intracellular growth in the early phase of primary infection. *Autophagy*. 2007;3(2):117–125.
- [8] Cullinane M, Gong L, Li X, et al. Stimulation of autophagy suppresses the intracellular survival of Burkholderia pseudomallei in mammalian cell lines. *Autophagy*. 2008;4(6):744–753.
- [9] Bressler AM, Kaye KS, LiPuma JJ, et al. Risk factors for Burkholderia cepacia complex bacteremia among intensive care unit patients without cystic fibrosis: a case-control study. *Infect Control Hosp Epidemiol*. 2007;28(8):951–958.
- [10] Drevinek P, Mahenthiralingam E. Burkholderia cenocepacia in cystic fibrosis: epidemiology and molecular mechanisms of virulence. *Clin Microbiol Infect*. 2010;16(7):821–830.
- [11] Ganesan S, Sajjan US. Host evasion by Burkholderia cenocepacia. *Front Cell Infect Microbiol*. 2011;1:25.
- [12] Lamothe J, Huynh KK, Grinstein S, et al. Intracellular survival of Burkholderia cenocepacia in macrophages is associated with a delay in the maturation of bacteria-containing vacuoles. *Cell Microbiol*. 2007;9(1):40–53.
- [13] Al-Khodori S, Marshall-Batty K, Nair V, et al. Burkholderia cenocepacia J2315 escapes to the cytosol and actively subverts autophagy in human macrophages. *Cell Microbiol*. 2014;16(3):378–395.
- [14] Assani K, Tazi MF, Amer AO, et al. IFN-gamma stimulates autophagy-mediated clearance of Burkholderia cenocepacia in human cystic fibrosis macrophages. *PLoS One*. 2014;9(5):e96681.
- [15] Kayagaki N, Warming S, Lamkanfi M, et al. Non-canonical inflammasome activation targets caspase-11. *Nature*. 2011;479(7371):117–121.
- [16] Akhter A, Caution K, Abu Khweek A, et al. Caspase-11 promotes the fusion of phagosomes harboring pathogenic bacteria with lysosomes by modulating actin polymerization. *Immunity*. 2012;37(1):35–47.
- [17] Casson CN, Copenhaver AM, Zwack EE, et al. Caspase-11 activation in response to bacterial secretion systems that access the host cytosol. *PLoS Pathog*. 2013;9(6):e1003400.
- [18] Aachoui Y, Leaf IA, Hagar JA, et al. Caspase-11 protects against bacteria that escape the vacuole. *Science*. 2013;339(6122):975–978.
- [19] Rosales-Reyes R, Aubert DF, Tolman JS, et al. Burkholderia cenocepacia type VI secretion system mediates escape of type II secreted proteins into the cytoplasm of infected macrophages. *PLoS One*. 2012;7(7):e41726.
- [20] Gavrillin MA, Abdelaziz DH, Mostafa M, et al. Activation of the pyrin inflammasome by intracellular Burkholderia cenocepacia. *J Immunol*. 2012;188(7):3469–3477.
- [21] Saitoh T, Fujita N, Jang MH, et al. Loss of the autophagy protein Atg16L1 enhances endotoxin-induced IL-1 β production. *Nature*. 2008;456(7219):264–268.
- [22] Lee J, Kim HR, Quinley C, et al. Autophagy suppresses interleukin-1 β (IL-1 β) signaling by activation of p62 degradation via lysosomal and proteasomal pathways. *J Biol Chem*. 2012;287(6):4033–4040.
- [23] Shi CS, Shenderov K, Huang NN, et al. Activation of autophagy by inflammatory signals limits IL-1 β production by targeting ubiquitinated inflammasomes for destruction. *Nat Immunol*. 2012;13(3):255–263.
- [24] Byrne BG, Dubuisson JF, Joshi AD, et al. Inflammasome components coordinate autophagy and pyroptosis as macrophage responses to infection. *MBio*. 2013;4(1):e00620–12.
- [25] Caution K, Gavrillin MA, Tazi M, et al. Caspase-11 and caspase-1 differentially modulate actin polymerization via RhoA and Slingshot proteins to promote bacterial clearance. *Sci Rep*. 2015;5:18479.
- [26] Harrison RE, Bucci C, Vieira OV, et al. Phagosomes fuse with late endosomes and/or lysosomes by extension of membrane protrusions along microtubules: role of Rab7 and RILP. *Mol Cell Biol*. 2003;23(18):6494–6506.
- [27] Hagar JA, Powell DA, Aachoui Y, et al. Cytoplasmic LPS activates caspase-11: implications in TLR4-independent endotoxic shock. *Science*. 2013;341(6151):1250–1253.
- [28] Shi J, Zhao Y, Wang Y, et al. Inflammatory caspases are innate immune receptors for intracellular LPS. *Nature*. 2014;514(7521):187–192.
- [29] Lamkanfi M, Kanneganti TD, Van Damme P, et al. Targeted peptide-centric proteomics reveals caspase-7 as a substrate of the caspase-1 inflammasomes. *Mol Cell Proteomics*. 2008;7(12):2350–2363.
- [30] Akhter A, Gavrillin MA, Frantz L, et al. Caspase-7 activation by the Nlr4/IpaF inflammasome restricts Legionella pneumophila infection. *PLoS Pathog*. 2009;5(4):e1000361.
- [31] Xu H, Yang J, Gao W, et al. Innate immune sensing of bacterial modifications of Rho GTPases by the pyrin inflammasome. *Nature*. 2014;513(7517):237–241.
- [32] Aubert DF, Xu H, Yang J, et al. A Burkholderia type VI effector deamidates Rho GTPases to activate the pyrin inflammasome and trigger inflammation. *Cell Host Microbe*. 2016;19(5):664–674.
- [33] Feng Y, Press B, Wandinger-Ness A. Rab 7: an important regulator of late endocytic membrane traffic. *J Cell Biol*. 1995;131(6 Pt 1):1435–1452.
- [34] Press B, Feng Y, Hoflack B, et al. Mutant Rab7 causes the accumulation of cathepsin D and cation-independent mannose 6-phosphate receptor in an early endocytic compartment. *J Cell Biol*. 1998;140(5):1075–1089.
- [35] Gutierrez MG, Munafò DB, Beron W, et al. Rab7 is required for the normal progression of the autophagic pathway in mammalian cells. *J Cell Sci*. 2004;117(Pt13):2687–2697.
- [36] Li J, Brierher WM, Scimone ML, et al. Caspase-11 regulates cell migration by promoting Aip1-cofilin-mediated actin depolymerization. *Nat Cell Biol*. 2007;9(3):276–286.
- [37] Aguilera MO, Beron W, Colombo MI. The actin cytoskeleton participates in the early events of autophagosome formation upon starvation induced autophagy. *Autophagy*. 2012;8(11):1590–1603.

- [38] Hagar JA, Miao EA. Detection of cytosolic bacteria by inflammatory caspases. *Curr Opin Microbiol.* 2014;17:61–66.
- [39] Bast A, Krause K, Schmidt IH, et al. Caspase-1-dependent and -independent cell death pathways in *Burkholderia pseudomallei* infection of macrophages. *PLoS Pathog.* 2014;10(3):e1003986.
- [40] Wang S, Miura M, Jung YK, et al. Murine caspase-11, an ICE-interacting protease, is essential for the activation of ICE. *Cell.* 1998;92(4):501–509.
- [41] Tazi MF, Dakhllallah DA, Caution K, et al. Elevated Mirc1/Mir17–92 cluster expression negatively regulates autophagy and CFTR (cystic fibrosis transmembrane conductance regulator) function in CF macrophages. *Autophagy.* 2016;12(11):2026–2037.
- [42] Zhao Z, Fux B, Goodwin M, et al. Autophagosome-independent essential function for the autophagy protein Atg5 in cellular immunity to intracellular pathogens. *Cell Host Microbe.* 2008;4(5):458–469.
- [43] Castillo EF, Dekonenko A, Arko-Mensah J, et al. Autophagy protects against active tuberculosis by suppressing bacterial burden and inflammation. *Proc Natl Acad Sci U S A.* 2012;109(46):E3168–76.
- [44] Jiang F, Wang X, Wang B, et al. The *Pseudomonas aeruginosa* type VI secretion PGAP1-like effector induces host autophagy by activating endoplasmic reticulum stress. *Cell Rep.* 2016;16(6):1502–1509.
- [45] Yu Y, Fang L, Zhang Y, et al. VgrG2 of type VI secretion system 2 of *Vibrio parahaemolyticus* induces autophagy in macrophages. *Front Microbiol.* 2015;6:168.
- [46] Bucci C, Thomsen P, Nicoziani P, et al. Rab7: a key to lysosome biogenesis. *Mol Biol Cell.* 2000;11(2):467–480.
- [47] Vanlandingham PA, Ceresa BP. Rab7 regulates late endocytic trafficking downstream of multivesicular body biogenesis and cargo sequestration. *J Biol Chem.* 2009;284(18):12110–12124.
- [48] Jager S, Bucci C, Tanida I, et al. Role for Rab7 in maturation of late autophagic vacuoles. *J Cell Sci.* 2004;117(Pt 20):4837–4848.
- [49] Kjos I, Borg Distefano M, Saetre F, et al. Rab7b modulates autophagic flux by interacting with Atg4B. *EMBO Rep.* 2017;18(10):1727–1739.
- [50] Jaber N, Mohd-Naim N, Wang Z, et al. Vps34 regulates Rab7 and late endocytic trafficking through recruitment of the GTPase activating protein armus. *J Cell Sci.* 2016.
- [51] Byfield MP, Murray JT, Backer JM. hVps34 is a nutrient-regulated lipid kinase required for activation of p70 S6 kinase. *J Biol Chem.* 2005;280(38):33076–33082.
- [52] Nobukuni T, Joaquin M, Rocco M, et al. Amino acids mediate mTOR/raptor signaling through activation of class 3 phosphatidylinositol 3OH-kinase. *Proc Natl Acad Sci U S A.* 2005;102(40):14238–14243.
- [53] Carroll B, Mohd-Naim N, Maximiano F, et al. The TBC/RabGAP armus coordinates Rac1 and Rab7 functions during autophagy. *Dev Cell.* 2013;25(1):15–28.
- [54] Kochl R, Hu XW, Chan EY, et al. Microtubules facilitate autophagosome formation and fusion of autophagosomes with endosomes. *Traffic.* 2006;7(2):129–145.
- [55] Fass E, Shvets E, Degani I, et al. Microtubules support production of starvation-induced autophagosomes but not their targeting and fusion with lysosomes. *J Biol Chem.* 2006;281(47):36303–36316.
- [56] Jahreiss L, Menzies FM, Rubinsztein DC. The itinerary of autophagosomes: from peripheral formation to kiss-and-run fusion with lysosomes. *Traffic.* 2008;9(4):574–587.
- [57] Mann SS, Hammarback JA. Molecular characterization of light chain 3. A microtubule binding subunit of MAP1A and MAP1B. *J Biol Chem.* 1994;269(15):11492–11497.
- [58] Kouno T, Mizuguchi M, Tanida I, et al. Solution structure of microtubule-associated protein light chain 3 and identification of its functional subdomains. *J Biol Chem.* 2005;280(26):24610–24617.
- [59] Aplin A, Jasionowski T, Tuttle DL, et al. Cytoskeletal elements are required for the formation and maturation of autophagic vacuoles. *J Cell Physiol.* 1992;152(3):458–466.
- [60] Marion S, Hoffmann E, Holzer D, et al. Ezrin promotes actin assembly at the phagosome membrane and regulates phago-lysosomal fusion. *Traffic.* 2011;12(4):421–437.
- [61] Ridley AJ, Hall A. The small GTP-binding protein rho regulates the assembly of focal adhesions and actin stress fibers in response to growth factors. *Cell.* 1992;70(3):389–399.
- [62] Mizuno K. Signaling mechanisms and functional roles of cofilin phosphorylation and dephosphorylation. *Cell Signal.* 2013;25(2):457–469.
- [63] Mi N, Chen Y, Wang S, et al. CapZ regulates autophagosomal membrane shaping by promoting actin assembly inside the isolation membrane. *Nat Cell Biol.* 2015;17(9):1112–1123.
- [64] Hamad MA, Skeldon AM, Valvano MA. Construction of aminoglycoside-sensitive *Burkholderia cenocepacia* strains for use in studies of intracellular bacteria with the gentamicin protection assay. *Appl Environ Microbiol.* 2010;76(10):3170–3176.
- [65] Abdulrahman BA, Khweek AA, Akhter A, et al. Depletion of the ubiquitin-binding adaptor molecule SQSTM1/p62 from macrophages harboring cfr deltaF508 mutation improves the delivery of *Burkholderia cenocepacia* to the autophagic machinery. *J Biol Chem.* 2013;288(3):2049–2058.
- [66] Amer A, Franchi L, Kanneganti TD, et al. Regulation of Legionella phagosome maturation and infection through flagellin and host Ipaf. *J Biol Chem.* 2006;281(46):35217–35223.
- [67] Lamkanfi M, Amer A, Kanneganti TD, et al. The nod-like receptor family member naip5/birc1e restricts Legionella pneumophila growth independently of caspase-1 activation. *J Immunol.* 2007;178(12):8022–8027.